Polarized Raman Spectroscopy Strategy for Molecular Orientation of Polymeric Fibers with Raman Tensors Deviating from the Molecular Frame

Citation for the original published paper (version of record):
Svenningsson, L., Evenäs, L. (2020). Polarized Raman Spectroscopy Strategy for Molecular Orientation of Polymeric Fibers with Raman
Tensors Deviating from the Molecular Frame. ACS Applied Polymer Materials, 2(11): 4809-4813.
http://dx.doi.org/10.1021/acsapm.0c00762

ACS APPLIED POLYMER MATERIALS

pubs.acs.org/acsapm

Article

Polarized Raman Spectroscopy Strategy for Molecular Orientation of Polymeric Fibers with Raman Tensors Deviating from the Molecular Frame

Leo Svenningsson* and Lars Nordstierna

Cite This: *ACS Appl. Polym. Mater.* 2020, 2, 4809−4813

Read Online

ACCESS | Metrics & More | Article Recommendations

ABSTRACT: Polarized light is frequently used to identify molecular anisotropy in polymers, biological systems, and other materials. The influence of the Raman tensor by polarized light reveals not only the chemical structure but also information on the morphology of polymers. The orientation distribution of molecules in polymers has previously been determined for systems with the principal axis components of the Raman tensor parallel to the molecular frame. In many cases, the Raman tensor principal axis is not parallel to the molecular chain axis. Therefore, the orientation of the Raman tensor, relative to the molecular chain axis, is crucial if accurate information about the molecular orientation distribution is sought for. This work presents a strategy for separating the Raman tensor orientation angles from the molecular orientation angles for polymeric samples with fiber symmetry. Composite polymeric materials often experience signal overlap in the X-ray scattering wide-angle region, where the anisotropy is often resolved. While X-ray scattering investigates intermolecular distances, Raman spectroscopy resolves chemical information, and anisotropy, by the influence of Raman scattering. The quantitative principles presented here may aid in the evaluation of anisotropy in such composite materials.

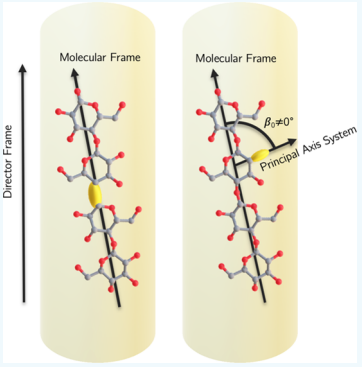

KEYWORDS: *Raman spectroscopy, molecular orientation distribution, Raman tensor, polymer, fiber, composite materials*

INTRODUCTION

Polarized Raman spectroscopy is an essential technique to measure molecular anisotropy in materials, with the most accessible method being the measurement of fractional scattered intensity $I_{\perp}/I_{\parallel}$. For determining the molecular orientation distribution in polymeric fibers, there is a handful of different experimental pathways, which analyze the nature of the Raman scattering tensor.[1−9] These methods are all based on Bower's seminal work (from 1972) on molecular orientation distribution measurements and all of which share one important limitation. The underlying model assumes that the Raman scattering tensor is parallel to the molecular frame (MF).[1] One such example is illustrated in Figure 1.

Many Raman scattering modes in polymers do not have their respective principal vibration in the molecular chain direction of the polymer. A set of reference frames and their relations are visualized in Figure 2 with the PAS of the Raman scattering tensor, an arbitrarily chosen MF, the DF of the fiber, and the laboratory frame (LAB).

This work presents a general model to determine the molecular orientation distribution when the Raman scattering tensor does not coincide with the MF. Such cases are useful when analyzing the crowded spectra, which is typically a situation for composite materials. More importantly, Raman spectroscopy can resolve anisotropy in the cases where the X-ray scattering pattern of two polymers with similar intermolecular distances overlap.[10,11] In addition, the proposed method has the potential to follow changes in the Raman tensor orientation relative to the MF during stretching of polymeric fibers. The NMR spectroscopy chemical shielding/shift anisotropy (CSA) orientation relative to the MF has previously been observed to change during stretching of polyamide-6 yarns.[12] Both types of tensor interactions, CSA and Raman scattering, respectively, are strongly correlated with the underlying chemical bonds, which indicates that changes in the Raman scattering orientation relative to the MF may occur if the polymer is stretched.[13] Fourier-transform infrared spectroscopy and X-ray scattering have also previously been used to study the changes in the angles of the glycosidic linkage and hydrogen bonding of cellulose, closely related to the corresponding Raman modes.[14] The Raman tensor orientation relative to the MF has also been studied by Jasse

Received: July 20, 2020
Accepted: September 9, 2020
Published: September 24, 2020

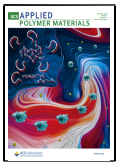

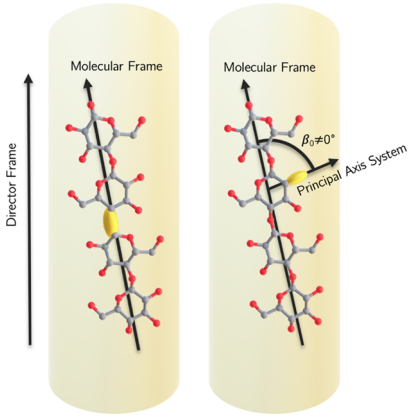

Figure 1. Visualization of the Raman tensor-related reference frames in a fiber with a short cellulose chain segment shown at an arbitrarily chosen angle deviation from the fiber axis, that is, director frame (DF). (Left) A Raman vibrational mode with the Raman principal axis system (PAS) tensor parallel to the MF, hence $\beta_0 = 0$. (Right) A Raman vibrational mode that is not parallel to the MF, hence $\beta_0 \neq 0$.

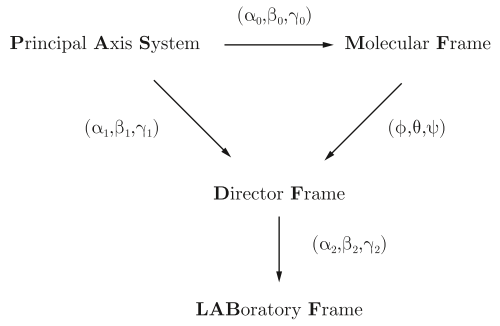

Figure 2. Notation of the reference frames for the polarized Raman experiment.

and Koenig by importing molecular information on polystyrene from IR and birefringence measurements.[15] The presented model in this work also has its use for structure illumination, drawing tangents to the work of Tsuboi et al. on biological systems.[16] Traditionally, orientation has been studied to determine its influence on tensile stress and creep resistance.[17] More recently, the orientational effects of electrically conducting polymers have been of increasing interest.[18−20]

RESULTS AND DISCUSSION

Bower's classical approach allows polarized light to interact with the Raman vibrational tensor and is subsequently analyzed through a polarization filter. The observed scattered intensity I_s has the form

$$I_s = I_0 \sum \left(\sum_{ij} l'_i l_j \alpha_{ij} \right)^2 \tag{1}$$

where l'_i is the scattered light vector through a polarization filter, l_j is the incident polarized light vector, and α is the Raman tensor. I_0 is dependent on the instrumental factors and the incident light intensity, and should be kept as a constant. The outside summation signifies the sum of a single vibrational mode from the contributions of all of the molecules in the light focus volume. When the scattered and incident light can come from all directions in the lab frame, the resulting quadratic expression can be written in the form $I_0 \sum \alpha_{ij} \alpha_{pq}$ from

$$I_s = I_0 \sum \left(\sum_{ij} l'_i l_j \alpha_{ij} \right) \left(\sum_{pq} l'_p l_q \alpha_{pq} \right) \tag{2}$$

where p and q are used to separate the coefficients of the quadratic expression. To reiterate on previous work, Bower showed that the scattered intensity can be written in the form of eq 3.

$$I_0 \sum \alpha_{ij}^{\mathrm{DF}} \alpha_{pq}^{\mathrm{DF}} = I_0 N_0 \int_0^{2\pi} \int_0^{\pi} \int_0^{2\pi} f(\theta) \alpha_{ij}^{\mathrm{DF}}(\phi, \theta, \psi) \alpha_{pq}^{\mathrm{DF}}(\phi, \theta, \psi) \sin\theta \, \mathrm{d}\phi \, \mathrm{d}\theta \, \mathrm{d}\psi \tag{3}$$

By using the tensor identity

$$\alpha_{ij}^{\mathrm{DF}}(\phi, \theta, \psi) = \sum_{k=1}^{3} a_{ik}(\phi, \theta, \psi) a_{jk}(\phi, \theta, \psi) \alpha_{kk}^{\mathrm{PAS}} \tag{4}$$

where a_{ik} is a component of a Euler rotational matrix, and $\alpha_{kk}^{\mathrm{PAS}}$ is a principal axis component of the Raman tensor in eq 5.

$$\alpha^{\mathrm{PAS}} = \begin{pmatrix} \alpha_{11}^{\mathrm{PAS}} & 0 & 0 \\ 0 & \alpha_{22}^{\mathrm{PAS}} & 0 \\ 0 & 0 & \alpha_{33}^{\mathrm{PAS}} \end{pmatrix} \tag{5}$$

The function $f(\theta)$ is the implied uniaxial orientation distribution function (ODF) of the polymer in a fiber. The constant N_0 is the number of polymer chain elements illuminated by the laser, where I_0 is the intensity of the laser. The ODF is only dependent on θ because there is uniaxial cylindrical symmetry around the angle ϕ. In addition, because the sample is assumed to contain many molecular chain elements, all of which have no rotational preference around the polymer's own chain axis, there is a rotational symmetry around the molecular chain axis with its Euler rotation as ψ. Polymers tend to contain local crystalline structures, which may have an orientation preference locally, but in a macroscopic sample, these crystallites are also uniformly distributed around ϕ and ψ. In Bower's model, the PAS Raman scattering tensor must coincide with the MF.[3−8] Hence, the Euler angles (ϕ, θ, and ψ), relevant to the polarized Raman experiments, describe the transformation directly from the PAS to the fiber DF. The molecular symmetries using Euler rotation are shown in Figure 3.

The requirement of the PAS parallel to MF limits the number of vibrational modes that can be quantitatively analyzed. The polarized Raman experiment can be rewritten in a more general form that allows for a Raman tensor orientation, which is not parallel to the MF. The series of Euler rotations that describe the Raman scattering tensor in the experimental reference frames, shown in Figure 2, are described by forward/active $Z-Y-Z$ rotations, following Bower's notation. To recall, an active $Z-Y-Z$ rotation describes the rotation of an object first by a rotation of ϕ around the Z-axis, second by a rotation of θ around the new Y-axis, and third by a rotation of ψ around the new Z-axis. Conversely, an identical complete rotation can be seen as a rotation of the coordinate system by first a rotation of ψ around the Z-axis, second a rotation of θ around the new Y-axis, and third by a rotation of ϕ around the new Z-axis.

https://dx.doi.org/10.1021/acsapm.0c00762
ACS Appl. Polym. Mater. 2020, 2, 4809−4813

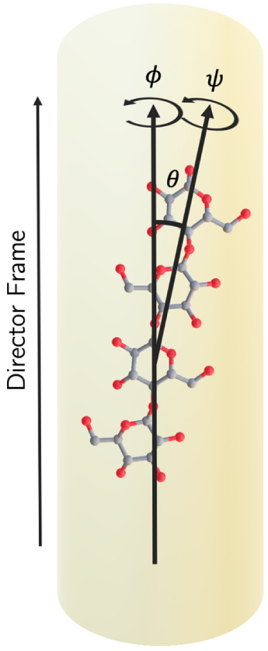

Figure 3. Visualization of the three Euler rotations between the MF and the DF. The polymer in the cylindrical fiber is in this case, the molecular structure of cellulose.

The active $Z-Y-Z$ Euler rotation matrix is described using eq 6.

$$\mathbf{R}_{\text{active}}(\phi, \theta, \psi) = \mathbf{R}_Z(\phi)\mathbf{R}_Y(\theta)\mathbf{R}_Z(\psi)$$
$$= \begin{pmatrix} \cos\phi & -\sin\phi & 0 \\ \sin\phi & \cos\phi & 0 \\ 0 & 0 & 1 \end{pmatrix} \begin{pmatrix} \cos\theta & 0 & \sin\theta \\ 0 & 1 & 0 \\ -\sin\theta & 0 & \cos\theta \end{pmatrix} \begin{pmatrix} \cos\psi & -\sin\psi & 0 \\ \sin\psi & \cos\psi & 0 \\ 0 & 0 & 1 \end{pmatrix} \tag{6}$$

The Raman scattering tensor in the reference frames in Figure 2 is described as

$$\boldsymbol{\alpha}^{\text{DF}} = \mathbf{R}(\alpha_1, \beta_1, \gamma_1)\boldsymbol{\alpha}^{\text{PAS}}\mathbf{R}^{-1}(\alpha_1, \beta_1, \gamma_1) \tag{7}$$

$$\boldsymbol{\alpha}^{\text{MF}} = \mathbf{R}(\alpha_0, \beta_0, \gamma_0)\boldsymbol{\alpha}^{\text{PAS}}\mathbf{R}^{-1}(\alpha_0, \beta_0, \gamma_0) \tag{8}$$

$$\boldsymbol{\alpha}^{\text{DF}} = \mathbf{R}(\phi, \theta, \psi)\boldsymbol{\alpha}^{\text{MF}}\mathbf{R}^{-1}(\phi, \theta, \psi) \tag{9}$$

By inserting eqs 8 into 9, we find a rotational equality between the PAS, MF, and DF systems

$$\mathbf{R}(\alpha_1, \beta_1, \gamma_1) = \mathbf{R}(\phi, \theta, \psi)\mathbf{R}(\alpha_0, \beta_0, \gamma_0) \tag{10}$$

with α_{ij}^{DF} describing a direct Euler rotation from the PAS to the DF, such as

$$\alpha_{ij}^{\text{DF}}(\alpha_1, \beta_1, \gamma_1) = [\mathbf{R}(\alpha_1, \beta_1, \gamma_1)\boldsymbol{\alpha}^{\text{PAS}}\mathbf{R}^{-1}(\alpha_1, \beta_1, \gamma_1)]_{ij} \tag{11}$$

The new perspective of eq 12 integrates over all molecular angles (ϕ, θ, ψ) relative to the DF to accommodate the molecular orientation distribution, as previously. However, the Raman tensor is described in the DF through an Euler transformation from the PAS. The Raman tensor components in the DF are then

$$I_0 \sum \alpha_{ij}^{\text{DF}}\alpha_{pq}^{\text{DF}} = I_0 N_0 \int_0^{2\pi}\int_0^{\pi}\int_0^{2\pi} f(\theta)\alpha_{ij}^{\text{DF}}(\alpha_1, \beta_1, \gamma_1)$$
$$\alpha_{pq}^{\text{DF}}(\alpha_1, \beta_1, \gamma_1)\sin\theta \, \mathrm{d}\phi \, \mathrm{d}\theta \, \mathrm{d}\psi \tag{12}$$

By expressing $\boldsymbol{\alpha}^{\text{DF}}$ in terms of its equivalent rotation from eq 10, we get

$$I_0 \sum \alpha_{ij}^{\text{DF}}\alpha_{pq}^{\text{DF}} = I_0 N_0 \int_0^{2\pi}\int_0^{\pi}\int_0^{2\pi} f(\theta)$$
$$[\mathbf{R}(\phi, \theta, \psi)\mathbf{R}(\alpha_0, \beta_0, \gamma_0)\alpha^{\text{PAS}}\mathbf{R}^{-1}(\alpha_0, \beta_0, \gamma_0)\mathbf{R}^{-1}(\phi, \theta, \psi)]_{ij}$$
$$[\mathbf{R}(\phi, \theta, \psi)\mathbf{R}(\alpha_0, \beta_0, \gamma_0)\alpha^{\text{PAS}}\mathbf{R}^{-1}(\alpha_0, \beta_0, \gamma_0)\mathbf{R}^{-1}(\phi, \theta, \psi)]_{pq}$$
$$\sin\theta \, \mathrm{d}\phi \, \mathrm{d}\theta \, \mathrm{d}\psi \tag{13}$$

The Raman tensor rotations are now divided into a rotation from PAS to MF $(\alpha_0, \beta_0, \gamma_0)$, and a rotation from MF to DF (ϕ, θ, ψ), which are the desired molecular orientation angles. The angle α_0 coincides with molecular rotational symmetry. For a sample with many semicrystalline molecular chain elements, as in a polymer, the angle α_0 can be chosen freely. In usual circumstances, it is convenient to set α_0 to 0 for computations. The unknown Euler angles β_0 and γ_0 can be determined either from experimental observation or computational modeling. Finally, the fiber sample is rotated around the lab frame in the direction of the incident light, which we choose to be the Y-axis, or the $\boldsymbol{x}_2$-axis in the LAB frame. The polarized Raman spectroscopy setup is shown in Figure 4 for both the back scattering and the right angle scattering experiments.

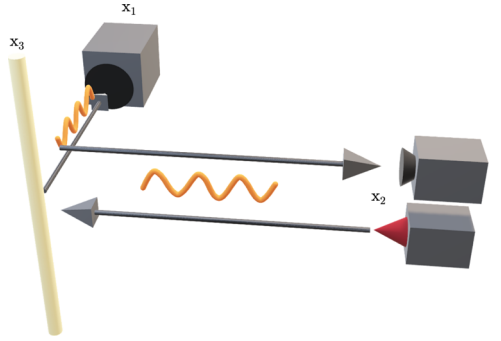

Figure 4. Schematic of the polarized Raman experiment on fibers with the laser entering in the $\mathbf{x}_2$ direction and exiting in the $\mathbf{x}_1$ direction for the right angle scattering geometry, while the laser is entering in the $\mathbf{x}_2$ direction and exiting at $\mathbf{x}_2$ for the back scattering geometry. The fiber is positioned in the $\mathbf{x}_1-\mathbf{x}_3$ plane with an angle β_2 that is parallel to $\mathbf{x}_3$ when $\beta_2 = 0$.

For most experimental setups, the incident light and detection directions are fixed to the LAB frame $\mathbf{x}_1$, $\mathbf{x}_2$, and $\mathbf{x}_3$ directions. The resulting possible experimental setups can then be simplified to eq 14

$$\mathbf{I}_{\text{s}}^{\text{LAB}} = I_0 \sum \boldsymbol{\alpha}^{\text{LAB}} \circ \boldsymbol{\alpha}^{\text{LAB}} \tag{14}$$

The general expression for both the back scattering and right angle scattering can be expressed as

$$\mathbf{I}_{\text{s}}^{\text{LAB}}(\beta_2) = I_0 \sum [\mathbf{R}_Y(\beta_2)\boldsymbol{\alpha}^{\text{DF}}\mathbf{R}_Y{}^{-1}(\beta_2)] \circ [\mathbf{R}_Y(\boldsymbol{\beta}_2)\boldsymbol{\alpha}^{\text{DF}}\mathbf{R}_Y{}^{-1}(\beta_2)] \tag{15}$$

from which all of the experimental scattering geometries can be derived. The angle β_2 corresponds to the Y-rotation of the fiber in the $\mathbf{x}_1-\mathbf{x}_3$ plane, with $\beta_2 = 0$ for a fiber in the $\mathbf{x}_3$ or Z-direction. For the three back scattering polarization configurations, corresponding to the matrix indices, eq 16 through 20 are obtained.

https://dx.doi.org/10.1021/acsapm.0c00762
ACS Appl. Polym. Mater. 2020, 2, 4809−4813

$$I_{33}^{BS}(\beta_2) = I_{33}^{RAS*}(\beta_2) = I_0 \sum (\alpha_{33}^{DF} \cos^2 \beta_2 - \alpha_{13}^{DF} \sin 2\beta_2 + \alpha_{11}^{DF} \sin^2 \beta_2)^2 \quad (16)$$

$$I_{11}^{BS}(\beta_2) = I_0 \sum (\alpha_{11}^{DF} \cos^2 \beta_2 + \alpha_{13}^{DF} \sin 2\beta_2 + \alpha_{33}^{DF} \sin^2 \beta_2)^2 \quad (17)$$

$$I_{13}^{BS}(\beta_2) = I_0 \sum \left(\alpha_{13}^{DF} \cos^2 \beta_2 + \frac{1}{2}\alpha_{33}^{DF} \sin 2\beta_2 - \frac{1}{2}\alpha_{11}^{DF} \sin 2\beta_2 - \alpha_{13}^{DF} \sin^2 \beta_2\right)^2 \quad (18)$$

$$I_{23}^{RAS}(\beta_2) = I_0 \sum (\alpha_{23}^{DF} \cos \beta_2 - \alpha_{21}^{DF} \sin \beta_2)^2 \quad (19)$$

$$I_{21}^{RAS}(\beta_2) = I_0 \sum (\alpha_{21}^{DF} \cos \beta_2 + \alpha_{23}^{DF} \sin \beta_2)^2 \quad (20)$$

BS and RAS refer to back scattering and right angle scattering experiments, respectively. The subscripts in $I_{ij}^{BS}(\beta)$ again refer to the polarization of the analyzer (i) and of the incident light (j), respectively. A common approximation to the Raman tensor sets the Raman tensor components to $\alpha_{11}^{PAS} = \alpha_{22}^{PAS}$, called the cylindrical tensor, which after careful consideration for certain molecular features can be introduced to reduce the number of unknown variables, thus decreasing the number of required experimental measurements.[3] The inclusion of a cylindrically symmetric tensor coincidentally also removes the need for a γ_0 rotation because it is a rotation around the α_{33}^{PAS} axis.

The choice of the ODF model $f(\theta)$ will affect the interpretation of the molecular order observed from experiments. The most commonly used ODF for fiber symmetries is the Legendre polynomials, for which the integral in eq 13 has an analytical solution. The Legendre polynomials, normalized over all Euler angles, are given using eq 21.

$$f(\theta) = \sum_{l=0}^{\infty} \frac{2l+1}{8\pi^2} \cdot \langle P_l \rangle \cdot P_l(\cos \theta) \quad (21)$$

Another approach is to use an ODF, which fits well for the specific material from other experimental observations, such as wide angle X-ray scattering and solid-state NMR spectroscopy.[9,13] In general, oriented materials do not adhere to a specific molecular orientation function, though in some cases a good enough approximation can be found.

Finally, the model provided by eq 13 was tested using the previously published data.[9] To make these newly added variables accessible for experimental studies, the test assumes cylindrically symmetric tensor $\alpha_{11}^{PAS} = \alpha_{22}^{PAS}$, which, as explained earlier, reduces the number of unknown variables to: α_{11}^{PAS}, α_{33}^{PAS}, β_0, and the ODF, $f(\theta)$. The ODF can be chosen to the Legendre polynomials, usually limited to P_2 and P_4 contributions, which leaves us five unknown variables as to be evaluated from experimental measurements.[1,3−6] The simplest experimental setup avoids the right angle scattering, hence requires that only 4 unknown variables are used with the complete (tilt) method. Notably, it is not possible to approximate the Legendre polynomials solely by P_2 using the complete (tilt) method because it leads to degenerate solutions.[9] Therefore, we have used data from a regenerated cellulose material, where the ODF has previously been well approximated by a periodic Lorentzian function instead of the Legendre polynomials.[9] When the set of equations could be solved with a minimized square sum, the angle $\beta_0 = 0$, and the order parameter $P_2 = 0.41$ after transforming the Lorentzian function to Legendre polynomials. The vibrational angle for the PAS to the MF β_0 suggests that the glycosidic C−O−C vibration is parallel to the MF. However, it should be noted that the effect of the cylindrically symmetric tensor approximation affects the measured order parameter for this selected sample with a change in the P_2 order parameter, from $P_2 = 0.50$ to $P_2 = 0.42$ in previous studies, and here obtained as $P_2 = 0.41$.

CONCLUSIONS

The separation of the Raman scattering tensor PAS and the MF allows additional Raman modes to be used to determine the molecular anisotropy in polymers. A plenitude of useable signals are needed when spectral features overlap. However, more importantly, Raman spectroscopy has the possibility to determine molecular anisotropy in the cases where X-ray scattering patterns of the composite materials overlap. The proposed strategy also allows monitoring the changes in the Raman tensor orientation relative to the MF. Such changes may occur in polymers during stretching from variations in the polymer bond angles and should in principle be accounted for in quantitative analysis.

AUTHOR INFORMATION

Corresponding Author

Leo Svenningsson − *Department of Chemistry and Chemical Engineering, Chalmers University of Technology, SE-41296 Göteborg, Sweden;* orcid.org/0000-0002-3813-347X; Email: leo.svenningsson@chalmers.se

Author

Lars Nordstierna − *Department of Chemistry and Chemical Engineering and Wallenberg Wood Science Center, Chalmers University of Technology, SE-41296 Göteborg, Sweden;* orcid.org/0000-0002-6580-0610

Complete contact information is available at: https://pubs.acs.org/10.1021/acsapm.0c00762

Notes

The authors declare no competing financial interest.

ACKNOWLEDGMENTS

This work has been carried out within the framework of the Avancell Center for Fiber Engineering and financially supported by "Södra Skogsägarna Foundation for Research, Development and Education". We would like to acknowledge Anna Martinelli for discussions.

REFERENCES

(1) Bower, D. I. Investigation of molecular orientation distributions by polarized Raman scattering and polarized fluorescence. *J. Polym. Sci., Polym. Phys. Ed.* **1972**, *10*, 2135−2153.

(2) Bower, D. I. Orientation distribution functions for uniaxially oriented polymers. *J. Polym. Sci., Polym. Phys. Ed.* **1981**, *19*, 93−107.

(3) Frisk, S.; Ikeda, R. M.; Chase, D. B.; Rabolt, J. F. Determination of the Molecular Orientation of Poly(propylene terephthalate) Fibers Using Polarized Raman Spectroscopy: A Comparison of Methods. *Soc. Appl. Spectrosc., Bull.* **2004**, *58*, 279−286.

(4) Citra, M. J.; Chase, D. B.; Ikeda, R. M.; Gardner, K. H. Molecular orientation of high-density polyethylene fibers characterized by polarized Raman spectroscopy. *Macromolecules* **1995**, *28*, 4007−4012.

(5) Yang, S.; Michielsen, S. Determination of the Orientation Parameters and the Raman Tensor of the 998 cm-1Band of Poly(ethylene terephthalate). *Macromolecules* **2002**, *35*, 10108−10113.
(6) Yang, S.; Michielsen, S. Orientation distribution functions obtained via polarized Raman spectroscopy of poly(ethylene terephthalate) fibers. *Macromolecules* **2003**, *36*, 6484−6492.
(7) Tanaka, M.; Young, R. J. Review Polarised Raman spectroscopy for the study of molecular orientation distributions in polymers. *J. Mater. Sci.* **2006**, *41*, 963−991.
(8) Richard-Lacroix, M.; Pellerin, C. Accurate New Method for Molecular Orientation Quantification Using Polarized Raman Spectroscopy. *Macromolecules* **2013**, *46*, 5561−5569.
(9) Svenningsson, L.; Lin, Y.-C.; Karlsson, M.; Martinelli, A.; Nordstierna, L. Molecular Orientation Distribution of Regenerated Cellulose Fibers Investigated with Polarized Raman Spectroscopy. *Macromolecules* **2019**, *52*, 3918−3924.
(10) Ureña-Benavides, E. E.; Kitchens, C. L. Wide-Angle X-ray Diffraction of Cellulose Nanocrystal-Alginate Nanocomposite Fibers. *Macromolecules* **2011**, *44*, 3478−3484.
(11) Abraham, E.; Elbi, P. A.; Deepa, B.; Jyotishkumar, P.; Pothen, L. A.; Narine, S. S.; Thomas, S. X-ray diffraction and biodegradation analysis of green composites of natural rubber/nanocellulose. *Polym. Degrad. Stab.* **2012**, *97*, 2378−2387.
(12) Schreiber, R.; Veeman, W. S.; Gabriëlse, W.; Arnauts, J. NMR Investigations of Orientational and Structural Changes in Polyamide-6 Yarns by Drawing. *Macromolecules* **1999**, *32*, 4647−4657.
(13) Svenningsson, L.; Sparrman, T.; Bialik, E.; Bernin, D.; Nordstierna, L. Molecular orientation distribution of regenerated cellulose fibers investigated with rotor synchronized solid state NMR spectroscopy. *Cellulose* **2019**, *26*, 4681−4692.
(14) Altaner, C. M.; Thomas, L. H.; Fernandes, A. N.; Jarvis, M. C. How Cellulose Stretches: Synergism between Covalent and Hydrogen Bonding. *Biomacromolecules* **2014**, *15*, 791−798.
(15) Jasse, B.; Koenig, J. L. Polarized Raman study of molecular orientation in uniaxially stretched atactic polystyrene. *J. Polym. Sci., Polym. Phys. Ed.* **1980**, *18*, 731−738.
(16) Tsuboi, M.; Benevides, J. M.; Thomas, G. J. Raman Tensors and their application in structural studies of biological systems. *Proc. Jpn. Acad., Ser. B* **2009**, *85*, 83−97.
(17) *Structure and Properties of Oriented Polymers*; Ward, I. M., Ed.; Springer-Science + Business Media, B.V., 1997.
(18) Lepinoy, M.; Limelette, P.; Schmaltz, B.; Van, F. T. Thermopower scaling in conducting polymers. *Sci. Rep.* **2020**, *10*, 8086.
(19) Kim, N.; Lienemann, S.; Petsagkourakis, I.; Mengistie, D. A.; Kee, S.; Ederth, T.; Gueskine, V.; Leclère, P.; Lazzaroni, R.; Crispin, X.; Tybrandt, K. Elastic conducting polymer composites in thermoelectric modules. *Nat. Commun.* **2020**, *11*, 1424.
(20) Hynynen, J.; Järsvall, E.; Kroon, R.; Zhang, Y.; Barlow, S.; Marder, S. R.; Kemerink, M.; Lund, A.; Müller, C. Enhanced Thermoelectric Power Factor of Tensile Drawn Poly(3-hexylthiophene). *ACS Macro Lett.* **2019**, *8*, 70−76.

https://dx.doi.org/10.1021/acsapm.0c00762
ACS Appl. Polym. Mater. 2020, 2, 4809−4813